

Exact Photoacoustic Image Reconstruction using a Planar Sensor Array and Image Sources

B. T. Cox and P. C. Beard

Department of Medical Physics and Bioengineering, University College London,
Gower Street, London WC1E 6BT, UK
www.medphys.ucl.ac.uk/research/mle

ABSTRACT

Photoacoustic imaging with planar sensor arrays suffers from a finite aperture or limited view problem due to the fact that the sensor array is finite in size, whereas exact reconstruction algorithms require that it occupies the entire infinite plane. Here, acoustic reflectors are proposed as a means of reflecting the acoustic waves, that would otherwise not be measured, back onto the sensor, and it is shown that an existing FFT-based image reconstruction algorithm can be used to reconstruct an image in this case without modification. A 2D simulation is used to show the improvement in the image quality when data from the reverberant field is included in the reconstruction. The improvement is explained by the matching of the periodicity implicitly assumed by the FFT algorithm and the periodicity in the virtual initial pressure distribution formed from the real initial pressure distribution and an infinite line of image sources generated by the acoustic reflectors.

Keywords: photoacoustic imaging, image reconstruction, reverberation, image sources

1. INTRODUCTION

In biomedical photoacoustic imaging of soft tissue, the initial pressure distribution due to impulsive heating following the absorption of a short laser pulse, generates acoustic waves (up to tens of MHz) which propagate to an acoustic sensor array surrounding or adjacent to the tissue. An imaging algorithm is then used to construct an image of the initial pressure distribution, which is proportional to the absorbed optical energy density and therefore related, via the absorption coefficient, to the constituent molecules of the tissue. Exact reconstruction algorithms are available for spherical,¹⁻³ cylindrical^{1,4,5} and planar geometries,^{1,6,7} although for exact reconstructions in the latter two cases the measurement surfaces must extend to infinity. It is the impracticality of infinitely wide sensor arrays, and the deleterious effects on the image quality of reconstructions with finite aperture arrays, that motivated this work, in which a reverberant cavity is used to extend the effective detection aperture.

2. REVERBERANT-FIELD PHOTOACOUSTIC IMAGING

In photoacoustic image reconstruction it is usual to assume that the acoustic waves travel from the source region, across the measurement surface (be it spherical, planar or whatever shape), and off to infinity. In other words, the reconstruction algorithms usually assume an acoustic free-field. In practice, the waves are reflected by the walls of the container surrounding the sample to be imaged, eg. the small animal or breast, and these reflections must be time-gated out to fulfill the free-field requirement. An alternative approach would be to include the acoustically reflecting boundaries in the model. ie. to remove the assumption of a free field and to take into account the reflections, thereby formulating reverberant-field image reconstruction algorithms. There are several advantages to this approach. First, the reflected acoustic waves may provide information that would otherwise have been lost; this is the case below in the case of a planar sensor array of finite extent. Second, the data can be measured over any length of time. This could be useful in situations where the noise is significant or signal very weak. For instance, using narrowband detection techniques, the reverberant field generated by a photoacoustic source modulated at a single-frequency at a time, eg. using a frequency chirp,

Send correspondence to B. T. Cox. bencox@mpb.ucl.ac.uk

Photons Plus Ultrasound: Imaging and Sensing 2007: The Eighth Conference on Biomedical Thermoacoustics, Optoacoustics, and Acousto-optics, edited by Alexander Oraevsky, Lihong V. Wang, Proc. of SPIE Vol. 6437, 64371H, (2007) · 1605-7422/07/\$18 · doi:10.1117/12.700006

could be measured over long time periods to improve the signal-to-noise ratio. Only through a reconstruction algorithm that includes the reflective effects of the boundaries could such measurements be used to form an image of the photoacoustic source. In the case of the planar sensor there are other advantages too, which are discussed further below.

3. IMAGE RECONSTRUCTION FROM PLANAR ARRAY MEASUREMENTS

Planar sensor arrays, consisting of piezoelectric or optical elements,⁸ are readily available and an efficient photoacoustic image reconstruction algorithm based on the Fast Fourier Transform (FFT) has been developed.^{6,7} Because, in practice, the sensor array is limited to making measurements over a finite region of the plane (Fig. 1), reconstructions with this algorithm suffer from blurring, sometimes called the ‘finite aperture effect’, or the ‘limited view’ or ‘partial scan’ problem. The blurring is caused by the loss of data when going from the infinite to the finite aperture case. Here we propose a method of overcoming this problem by reflecting the acoustic waves back onto the sensor array using two acoustic reflectors perpendicular to the sensor array. A schematic of this arrangement is shown in Fig. 2.

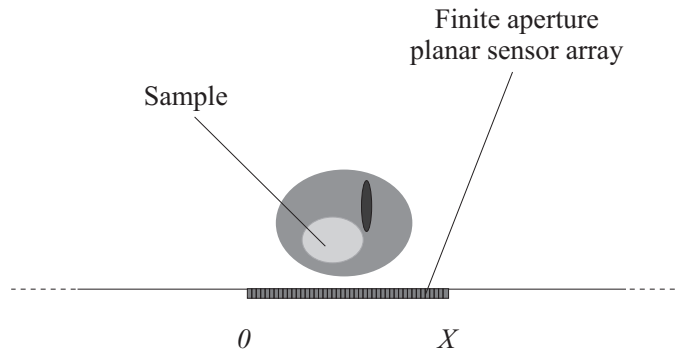


Figure 1. Conventional measurement configuration with a finite aperture planar sensor.

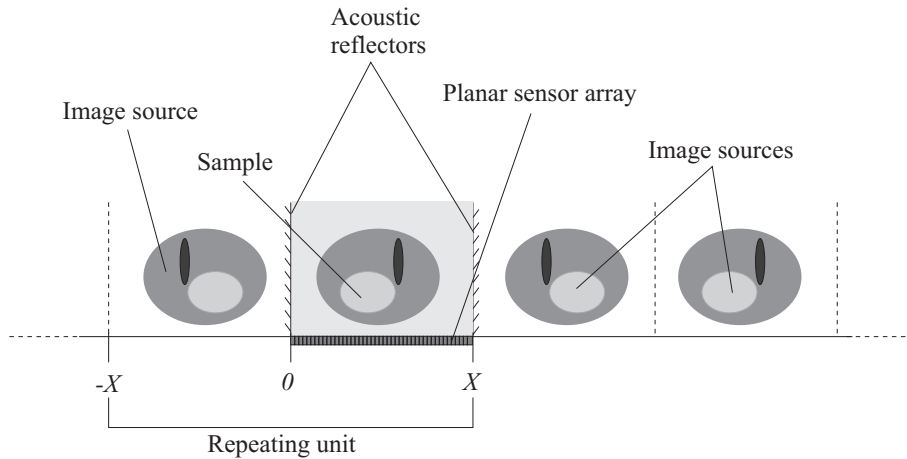


Figure 2. Measurement configuration consisting of two acoustically reflecting walls either side of the sample and perpendicular to the plane of the sensor array.

4. FFT PERIODICITY AND IMAGE SOURCES

In the reconstruction algorithm referred to above,^{6,7} one of the uses of the FFT is to transform the discrete, sampled, data in the spatial domain, $p(x)$, to discrete data in the wavenumber domain $p(k_x)$. The discreteness of the wavenumber domain representation of the signal implies that the original data in the spatial domain must have been periodic, or have come from a periodic sequence. (The FFT represents the signal as a sum of components at wavenumbers $\{0, \Delta k_x, 2\Delta k_x, 3\Delta k_x, \dots\}$, which are all multiples of the smallest non-zero wavenumber Δk_x , implying a periodicity in the original signal.) The implication is that the initial pressure distribution is periodic with period $X = 2\pi/\Delta k_x$. Of course, the initial pressure distribution, as shown in Fig. 1, is not periodic, and this is one way to explain the blurring due to the finite aperture effect in this case.

The FFT reconstruction algorithm is very efficient computationally, so we do not want to discard it, but how can this requirement for periodicity be satisfied, in order to reduce the blurring? The approach taken here is to introduce acoustic image sources, ie. reflections of the initial pressure distributions, thus generating a virtual initial pressure distribution which is periodic with a period of $2X$ (Fig. 2). The pressure data measured with the sensor array from 0 to X will be identical to the data that would be measured from 0 to $-X$, were there a sensor array there and were the image sources real. To match the periodicity of the virtual initial pressure distribution to the periodicity implicit in the FFT algorithm all that is required is that the vector of measured data $\{p(0), p(\Delta x), \dots, p(X - \Delta x), p(X)\}$ is used to form another vector of twice the length, for use in the image reconstruction algorithm, given by $\hat{p} = \{p(X), p(X - \Delta x), \dots, p(\Delta x), p(0), p(\Delta x), \dots, p(X)\}$. One additional requirement to ensure that \hat{p} really is periodic is that the first and last measurement points, 0 and X , lie a distance $\Delta x/2$ from the acoustic reflectors.

5. NUMERICAL SIMULATION

Figure 3 shows a two-dimensional simulation of this problem. While a 2D example is given here, the ideas can easily be extended to three dimensions, with four walls forming an open box. An initial pressure distribution consisting of a number of circles (top left image) was chosen so that the spatial variation of the degradation of the reconstructed image would be apparent. The pressure time series that such an initial pressure distribution would generate were simulated⁹ for a sensor array composed of 512 elements spaced evenly from $-10 < x < 10$ mm on the $y = 0$ plane. Time series were generated for the case without acoustic reflections (top right image in Fig. 3), and the case with acoustic reflections from perfectly-reflecting walls perpendicular to the sensor and positioned at $x = 10$ and -10 . The time series in the latter case were truncated at $14 \mu s$, corresponding approximately to the time over which the free-field signals are non-zero. Noise was added to both sets of data and images of the initial pressure distribution were formed using the FFT-based algorithm referred to above.^{6,10} The image generated using the data without reflections is shown in the bottom left image of Fig. 3 and the image formed from the data containing the reflections in the bottom right.

There is a clear improvement in the reconstruction even though the time series for the reverberant case were truncated at $14 \mu s$. When more of the reverberation is recorded, ie. when the time series are measured for a longer time, the image quality improves correspondingly. (The lighter vertical stripes in the image are thought to be due to the fact that the reconstruction algorithm neglects the evanescent part of the spectrum.) Even in this case two features are clear: the edges of the circles have been reconstructed more accurately, and the blurring depends only on y and no longer on x as well. This is because in the reverberant case the 'effective aperture width' depends on the length of time for which the reverberation has been recorded and every point in the image is central to this 'effective aperture', whereas in the free-field case the view of the sensor array is different from different points in the image. This reduction of the spatial variation of the blurring could have significant implications when deconvolving the effect of a sensor response from the image.

The image resolution and sharpness of the boundaries can be improved, in the reverberant case, by recording over a longer time period. In the free-field case, the image resolution can be improved only by enlarging the size of the sensor array. A significant advantage of the former is that it is cheaper; a disadvantage is that the target to be imaged must be small enough to fit within the reflecting walls, limiting targets to small animals, excised tissue, or the breast, for instance.

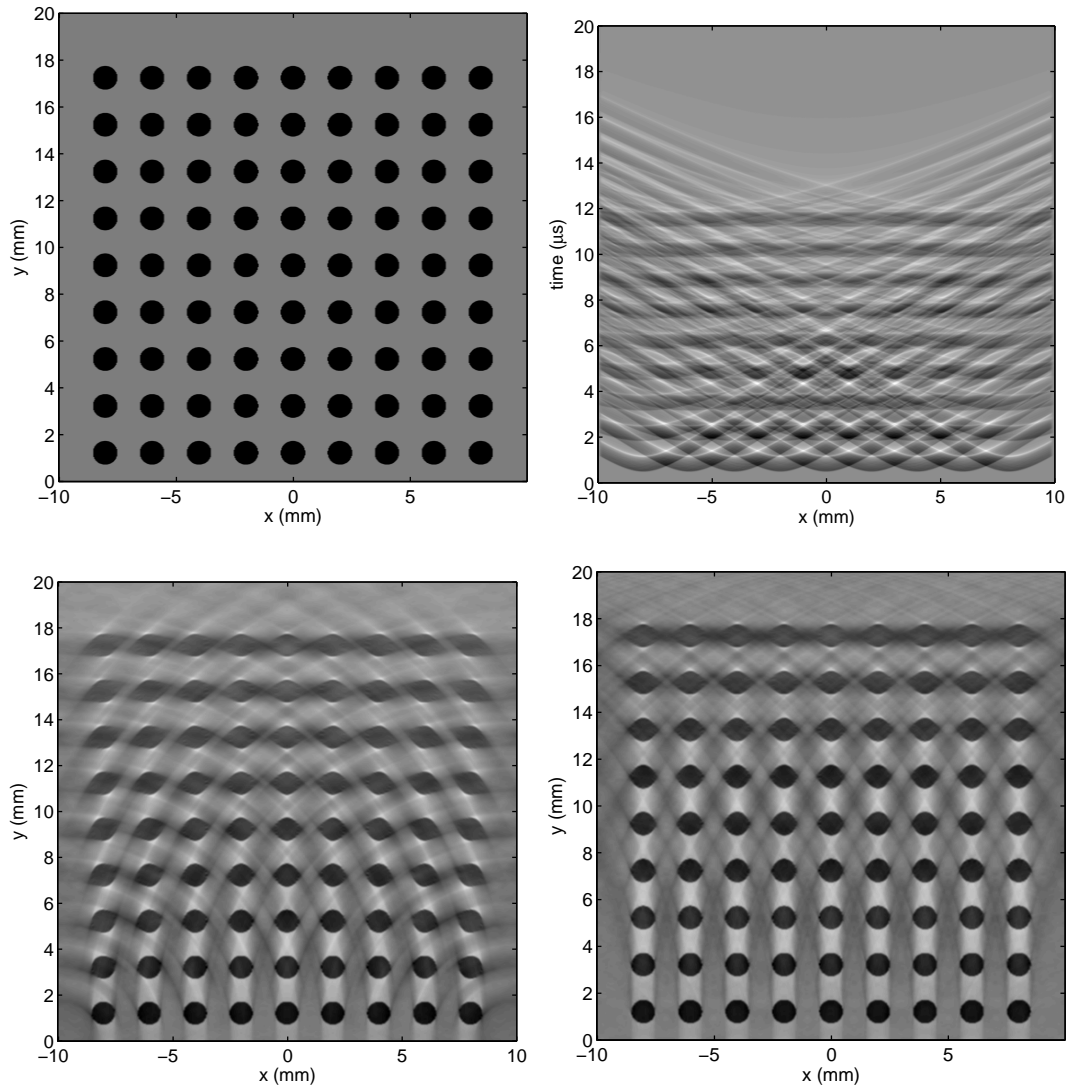


Figure 3. Top left: true initial pressure distribution. Top right: simulated time series of the acoustic pressure at the sensor located on the $y = 0$ plane between $-10 < x < 10$. Bottom left: Initial pressure distribution reconstructed from data recorded over a finite aperture and containing no acoustic reflections (the time series above). Bottom right: Initial pressure distribution reconstructed from reverberant field data recorded over $14 \mu\text{s}$ (time series not shown).

6. SUMMARY

In order to overcome the limitations due to the finite aperture effect, reverberant-field photoacoustic imaging is proposed, in which both the free-field and reverberant components of the acoustic field are used to generate the photoacoustic image. It has been shown that, for the particular case of a planar sensor with a pair acoustic reflectors mounted perpendicular to it, an existing algorithm based on the FFT can be used to reconstruct an image. Reflecting the acoustic waves, that would not usually be detected by the sensor array, back onto it, provides additional information for the image reconstruction, and results in images with fewer artefacts and improved spatial resolution.

ACKNOWLEDGMENTS

This work was supported by the Engineering and Physical Sciences Research Council, UK.

REFERENCES

1. S. J. Norton and M. Linzer, "Ultrasonic reflectivity imaging in 3 dimensions - exact inverse scattering solutions for plane, cylindrical, and spherical apertures," *IEEE Trans. Biomed. Eng.* **28**, pp. 202–220, 1981.
2. M. H. Xu and L. H. V. Wang, "Time-domain reconstruction for thermoacoustic tomography in a spherical geometry," *IEEE Trans. Med. Imag.* **21**(7), pp. 814–822, 2002.
3. D. Finch, S. K. Patch, and Rakesh, "Determining a function from its mean values over a family of spheres," *SIAM J. Math. Anal.* **35**, pp. 1213–1240, 2003.
4. Y. Xu, M. H. Xu, and L. H. V. Wang, "Exact frequency-domain reconstruction for thermoacoustic tomography - II: cylindrical geometry," *IEEE Trans. Med. Imag.* **21**(7), pp. 829–833, 2002.
5. S. J. Norton and T. Vo-Dinh, "Optoacoustic diffraction tomography: analysis of algorithms," *J. Opt. Soc. Am. A* **20**, pp. 1859–1866, 2003.
6. K. P. Köstli, M. Frenz, H. Bebie, and H. P. Weber, "Temporal backward projection of optoacoustic pressure transients using Fourier transform methods," *Phys. Med. Biol.* **46**(7), pp. 1863–1872, 2001.
7. Y. Xu, D. Z. Feng, and L. H. V. Wang, "Exact frequency-domain reconstruction for thermoacoustic tomography - I: planar geometry," *IEEE Trans. Med. Imag.* **21**(7), pp. 823–828, 2002.
8. E. Z. Zhang and P. C. Beard, "Broadband ultrasonic field mapping system using a wavelength tuned, optically scanned focussed beam to interrogate a Fabry-Perot polymer film sensor," *IEEE Trans. UFFC* **53**, pp. 1330–1338, 2006.
9. B. T. Cox and P. C. Beard, "k-space propagation models for acoustically heterogeneous media: application to biomedical photoacoustics," *J. Acoust. Soc. Am.*, accepted subject to revision, 2007.
10. K. Köstli and P. Beard, "Two-dimensional photoacoustic imaging by use of Fourier-transform image reconstruction and a detector with an anisotropic response," *Applied Optics* **42**(10), pp. 1899–1908, 2003.